Gaia DPAC
Data Processing & Analysis Consortium

Recommended initial spin phase for Gaia Scanning Law for the period until 31.12.2015

prepared by: S.A. Klioner, F. Mignard
affiliation : LO

reference: GAIA-C3-TN-LO-SK-022-1
issue: 1
revision: 1
date: 2014-09-01
status: Issued

Abstract

This technical note describes the justification for the choice of the initial spin phase to be used until the end of 2015:

$$\Omega_0 = 339.0^\circ\,.$$

This value of the initial spin phase is suitable for an investigation of the Gaia astrometric performance close to Jupiter and for the tests of algorithms and software for GAREQ. We stress that this value of Ω_0 is not suitable to reach the optimal accuracy of GAREQ. If no spin phase change is planned after December 2015, the final accuracy of GAREQ would be reduced by a significant factor.

Document History

Issue	Revision	Date	Author	Comment
1	1	2014-09-01	SK	A misprint in the link in Section 6 is fixed
1	0	2014-08-26	SK	Minor editing; issued to the Livelink
D	0	2014-08-25	FM	Check and minor editing
D	0	2014-08-23	SK	Start of the document

Contents

1 Notations **7**

2 Introduction **7**

3 Used parameters, models and data **8**

4 Investigation of the observations for $\nu_0 = 52.66°$ **9**

5 Recommendation of the initial spin phase till the end of 2015 **17**

6 Online repository **17**

A Comparison of the latest Gaia orbit with the orbit used to optimize the precession phase **18**

B Observations for $\nu_0 = 52.66°$ and $\Omega_0 = 339.0°$ till the end of 2015 **20**

C Time periods of GAREQ-relevant observations for $\nu_0 = 52.66°$ **22**

List of Figures

1 Total number of observations 11
2 Brightness of observed stars 11
3 Total s/n ratio for the monopole deflection 12
4 Total s/n ratio for the quadrupole deflection 12
5 S/n ratios for individual observations for the monopole deflection 13
6 S/n ratios for individual observations for the quadrupole deflection 13
7 Angular distances in arcseconds for all observations 14
8 Angular distances in Jupiter's radii for all observations 14
9 Total number of observations closer than 4 Jupiter radii 15
10 Characteristics of individual observations for $\Omega_0 = 339.0^\circ$ 16
11 Differences in Gaia position components between the MOC orbit files delivered on 19.08.2014 and 30.12.2013 19
12 Absolute difference in Gaia position between the MOC orbit files delivered on 19.08.2014 and 30.12.2013 19

List of Tables

1 Notations used in this document 7

Acronyms

The following table has been generated from the on-line Gaia acronym list:

Acronym	Description
2MASS	Two-Micron All Sky Survey
AC	across scan
AGIS	Astrometric Global Iterative Solution
AL	along scan
CCD	Charge-Coupled Device
CDS	Centre de Données astronomiques de Strasbourg (Strasbourg astronomical Data Center)
CPU	Central Processing Unit
DLR	Deutsches Zentrum für Luft und Raumfahrt
DPAC	Data Processing and Analysis Consortium
DPACE	Data Processing and Analysis Consortium Executive
DSS	Digitized Sky Survey
EPS	Electrical Power Sub-system
EPSL	Ecliptic Pole Scanning Law
ESA	European Space Agency
ESOC	European Space Operations Centre (ESA)
FOV	Field of View (also denoted FOV)
FoVRS	Field-of-View Reference System
GAREQ	GAia Relativistic Experiment on Quadrupole light deflection
GGU	Global Generic Update
GPDB	Gaia Parameter DataBase
GREM	Gaia RElativity Model
IOCR	In-Orbit Commissioning Review
JD	Julian Date
MOC	Mission Operations Centre
MSL	Modified Scanning Law
NSL	Nominal Scanning Law
PC	Project Coordinator
PO	Project Office
PS	Project Scientist
REMAT	RElativistic Models And Tests (DU in CU3)
RSLS	Reference Scanning Law Schedule
SL	Scanning Law
s/n	signal-to-noise (ratio)
SOC	Science Operation Centre
SOGAR	Scanning-law Optimization for GAREQ
TCB	Barycentric Coordinate Time
TDB	Barycentric Dynamical Time (obsolete)
TYC	TYCHO (stellar calatog)

References

F. Mignard, S.A. Klioner, Ch. Ordenovic, 2014, NSL Optimization for Quadrupole Experiment(SOGAR), GAIA-C3-TN-OCA-FM-050-D, in preparation

F. Mignard, Ch. Ordenovic, SOGAR Status Presentation at the REMAT-12 meeting, 11-12 July 2013. http://gaia.esac.esa.int/dpacsvn/DPAC/meetings/CU3/REMAT//12-Paris-Jul-13/FM_REMAT12_SOGAR.pdf

S.A. Klioner, F. Mignard, 2014, Recommended initial precession phase for Gaia Scanning Law, GAIA-C3-TN-TUD-SK-018-1, http://www.rssd.esa.int/cs/livelink/open/3238429

1 Notations

The main mathematical notations used in this report are summarized in Table 1.

Symbol	Meaning
ω	scan rate, arcsec/s (deg/h)
Ω	spin phase, degrees
Ω_0	initial spin phase at reference epoch, degrees
ν	precession phase, degrees
ν_0	initial precession phase at reference epoch, degrees
$T_{\rm ref}$	reference epoch for the initial phases: 1 Sep 2013, 0h TCB, JD = 2456536.5 TCB
s/n	a short-hand for the merit function or the efficiency factor

TABLE 1: Notations used in this document

2 Introduction

The optimization of the free NSL parameters for GAREQ observations is used to increase the overall s/n ratio for the quadrupole light deflection due to Jupiter. After the initial precession phase of the scanning law was fixed at 52.66° (Klioner & Mignard, 2014), the only remaining freedom in the NSL parameters is the initial spin phase. It was not possible to fix the initial spin phase simultaneously with the initial precession phase because at that time the final value of the scan rate was unknown. The scan rate value was fixed on 21 April 2014 (see below). However, because of the ongoing commissioning activities and the overall schedule of the mission, the GAREQ-optimized NSL with the precession phase of 52.66° is only used from the end of September 2014.

In principle, the impossibility to optimize simultaneously the initial precession and spin phases made the whole optimization procedure more complicated. However, it also led to the idea that the spin phase can be changed a few times during the mission to further increase the s/n ratio for the quadrupole light deflection. This idea was investigated in detail and some algorithms for the optimization of the spin phase during the mission were implemented and tested (Klioner & Mignard, 2014).

Clearly, during the optimization of the NSL parameters for GAREQ our current understanding of the Gaia performance when observing stars close to Jupiter was extensively used. The results of the optimization depend crucially on this performance. The three noise models N_1, N_2 and N_3 used for the optimization are described in Section 3.1 of Klioner & Mignard (2014). Although Gaia in-orbit commissioning did give some additional information on the Gaia performance it was not possible to obtain a sensitive update on the noise model up to now.

On the other hand, the SOGAR runs with the updated scan rate and the current Gaia orbit show that during 2015 there is no observations with the s/n ratio for the quadrupole deflection larger than 0.44 irrespectively of the selected initial spin phase (see Section 4). It means that this period of time is not very important for the quadrupole light deflection itself and can be used for other purposes.

Because of all these circumstances and the fact that a few spin phase changes during the mission are possible, it appears reasonable to use the observation time till September 2015 to gather more information on the actual performance of Gaia for observations close to Jupiter and then use this information for the GAREQ-relevant optimization of the NSL to be used starting from 2016. This nicely agreed with the request from the SOC and PO to first deliver the initial spin phase for the time period till the end of 2015.

The present technical note describes the results of the optimization of the initial spin phase to be used until 31 December 2015. The goals of the optimization were to maximize the potential outcome for the investigation of the noise model close to Jupiter and to ensure that some observations in 2014–2015 can be used for the training for the future differential solution for GAREQ. Both goals suggest to maximize the number of observations of relatively bright stars as close as possible to Jupiter.

3 Used parameters, models and data

1. The scan rate in this report was fixed to the finally selected scan rate of Gaia as delivered in the corresponding xml file by the SOC:

$$\omega_{\mathrm{TDB}} = 0.0002906967072617\ \mathrm{rad/s} = 59.9605000000034385\ \mathrm{arcsec/s}. \quad (1)$$

   According to the comments in the XML file the optimal value was found on 21 April 2014. Since SOGAR as all DPAC software works in TCB we need to convert this value into a TCB-compatible quantity:

$$\omega_{\mathrm{TCB}} = 59.9604990703040330588 61\ \mathrm{arcsec/s}. \quad (2)$$

2. In this report the initial precession phase was considered as fixed to $\nu_0 = 52.66^\circ$ as recommended in Klioner & Mignard (2014).

3. To be compatible with Klioner & Mignard (2014) we use the same mission duration and the stating epoch of observations as described in Section 6.1 of Klioner & Mignard (2014). However, only observations till the end of 2015 were considered (see Section 4).

4. For the SOGAR runs used for the spin phase optimization described in this report, the Gaia orbit as `ORB1_20140819_000001.txt` delivered on 19 August 2014 was used (see Appendix A).

5. The noise models N_1, N_2 and N_3 used to estimate the astrometric accuracy of the observations close to Jupiter are described in Section 3.1 of Klioner & Mignard (2014). For some of the plots in this technical note the model N_1 is used (see below).

4 Investigation of the observations for $\nu_0 = 52.66°$

We started with generating with SOGAR all observations until 31.12.2015 for $\nu_0 = 52.66°$ with the final scan rate and with the spin phase sampled from 0 to 360° with a step 0.25°. All observations within 10 Jupiter radii were considered (not limiting the minimal distance to Jupiter).

We noticed that the optimization of the number of observations as close as possible to Jupiter tended to select observations taking place very close to the edges of the FoVs. To lessen the danger of relying only on those observations two versions of the data were considered: with full FoVs (the shrink factor is set to 1.0 in SOGAR) and with the AC extension of the FoVs artificially reduced by 10% (a customizable shrink factor in SOGAR settings was set to 0.9).

All plots on Figures 1–9 show a quantity or quantities as function of the initial spin phase. In all cases all observations till the end of 2015 within at most 10 Jupiter radii are considered. Figure 1 shows the total number of observations. Figure 2 shows all magnitudes of stars observed for each initial spin phase. Figures 3–4 give the total s/n ratio from all these observations for the monopole and quadrupole light deflection, respectively. Figures 5–6 give the s/n ratios for individual observations for the monopole and quadrupole light deflection, respectively. For all plots of the s/n ratios the noise model N_1 is used. Finally, Figures 7–8 give the angular distances for all observations of all stars expressed in arcseconds and in apparent Jupiter's radii (computed for each observation).

We can see that whatever the initial spin phase there are no observations closer than 2 Jupiter's radii. Irrespectively of the initial spin phase the maximal possible s/n ratio for the quadrupole deflection of light for one observation does not exceed 0.44. These circumstances lead to the idea to reconsider the merit of each observations and optimize simply for the number of observations closer to Jupiter than 4 radii. This will allow us to test the noise level when stars are crossing the FoV in the immediate vicinity of Jupiter. The number of such observations for all initial spin phases are shown in Figure 9. One immediately sees that the initial spin phases in the range between 312.25° and 339.50° with a total of 7 observations even with the shrink factor 0.9 become interesting. On the other hand, Figure 5 shows that in this range the monopole deflection s/n ratio for the best observation increases with the initial spin phase. This means that the initial spin phase of around 339.50° is close to the optimal choice.

This hypothesis was further investigated using a different sort of plots shown on Figure 10. For each value of the initial spin phase Ω_0 we depict all observation till the end of 2015 and within 10 radii of Jupiter as a circle. The position of this circle is defined by the angular distance in

Jupiter's radii at which a star was observed (x-axis) and the magnitude of that star (y-axis). The color of the circle corresponds to the time of observation as shown at the bottom of the Figure 10. The plot on Figure 10 remains the same for the shrink factors 0.9 and 1.0. Similar plots were generated for all values of Ω_0 from 0° to 360° with a step of 0.25°. Then from these plots two animations were produced for the shrink factor 1.0 and 0.9. The animations as well as individual plots are available from the online repository (Section 6). The animations and frame-by-frame viewing allowed us to conclude that the value $\Omega_0 = 339.0^\circ$ is the most optimal one. The choice of 339.0° over 339.5° is somewhat arbitrary. At $\Omega_0 > 339.5^\circ$ one looses one observation within 4 radii of Jupiter, but only with the shrink factor 0.9. The value 0.9 is itself arbitrary and could be chosen a bit larger. The observation that would be lost with the shrink factor 0.9 is not the best one, but that of a star of magnitude 14.6 at about 3.3 radii of Jupiter. On the other hand, it is not clear how accurate a spin phase maneuver can be executed. Taking in account all these circumstances, it was decided to select the value $\Omega_0 = 339.0^\circ$. The observations that can be expected with this value of the initial spin phase till the end of 2015 are given in Appendix B.

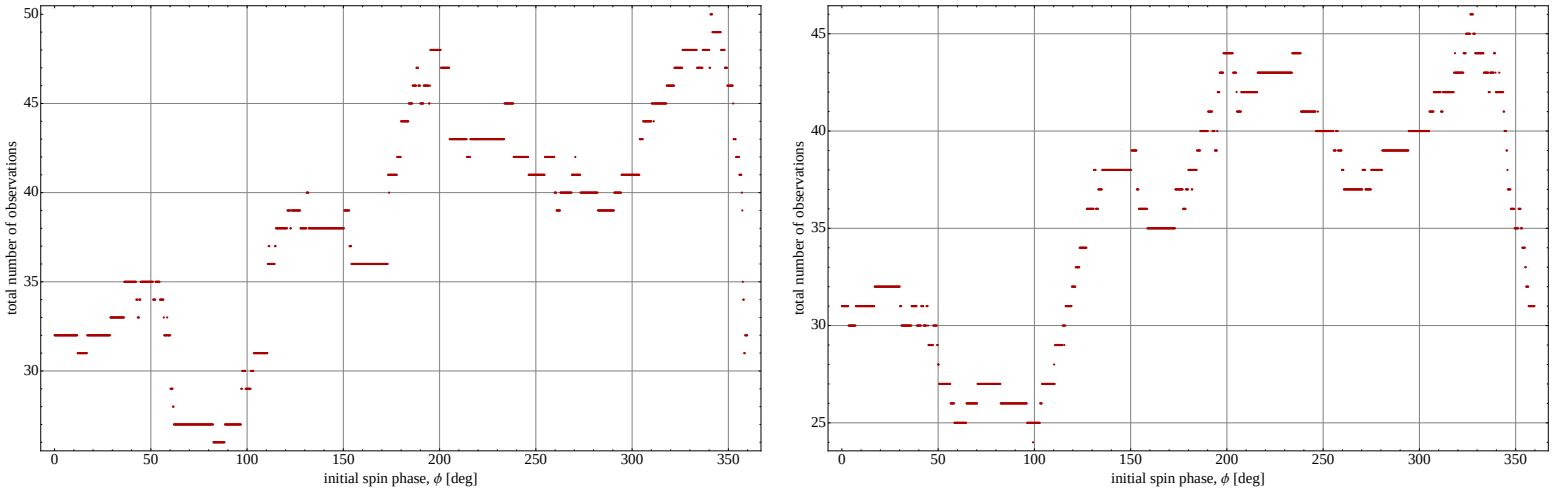


FIGURE 1: Total number of observations till 31.12.2015 within 10 Jupiter radii. The left pane with full FoVs, the right pane with the shrink factor 0.9.

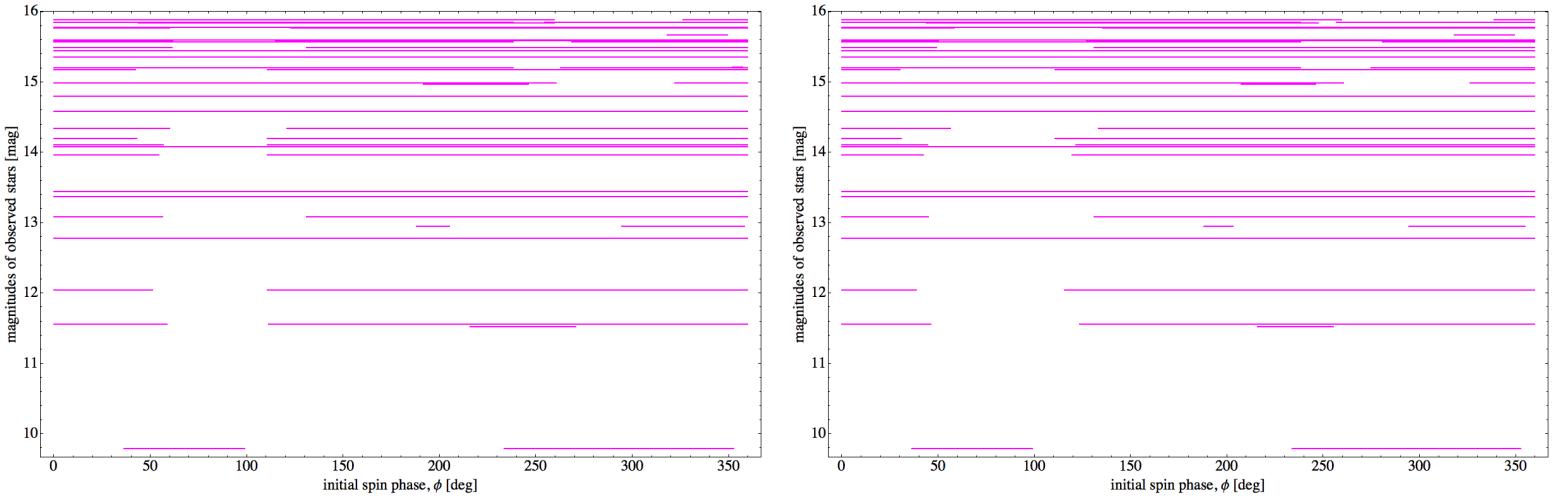


FIGURE 2: Brightness of all stars observed till 31.12.2015 within 10 Jupiter radii. The left pane with full FoVs, the right pane with the shrink factor 0.9.

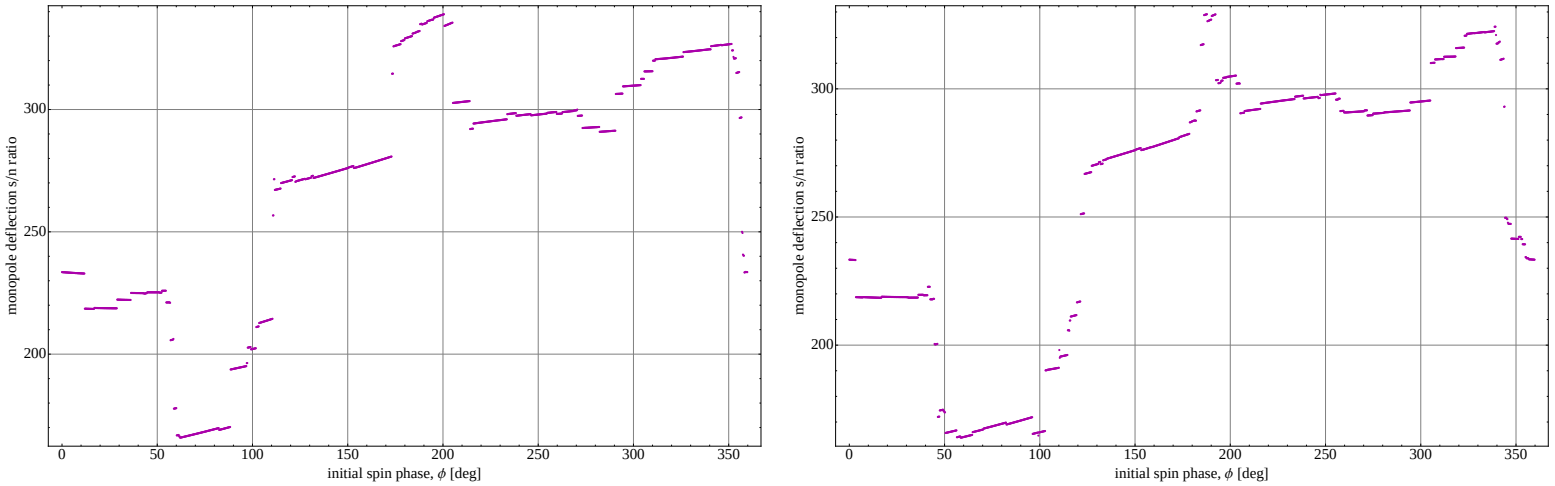


FIGURE 3: Total s/n ratio for the monopole deflection for all observations till 31.12.2015 within 10 Jupiter radii. The noise model N_1 was used. The left pane with full FoVs, the right pane with the shrink factor 0.9.

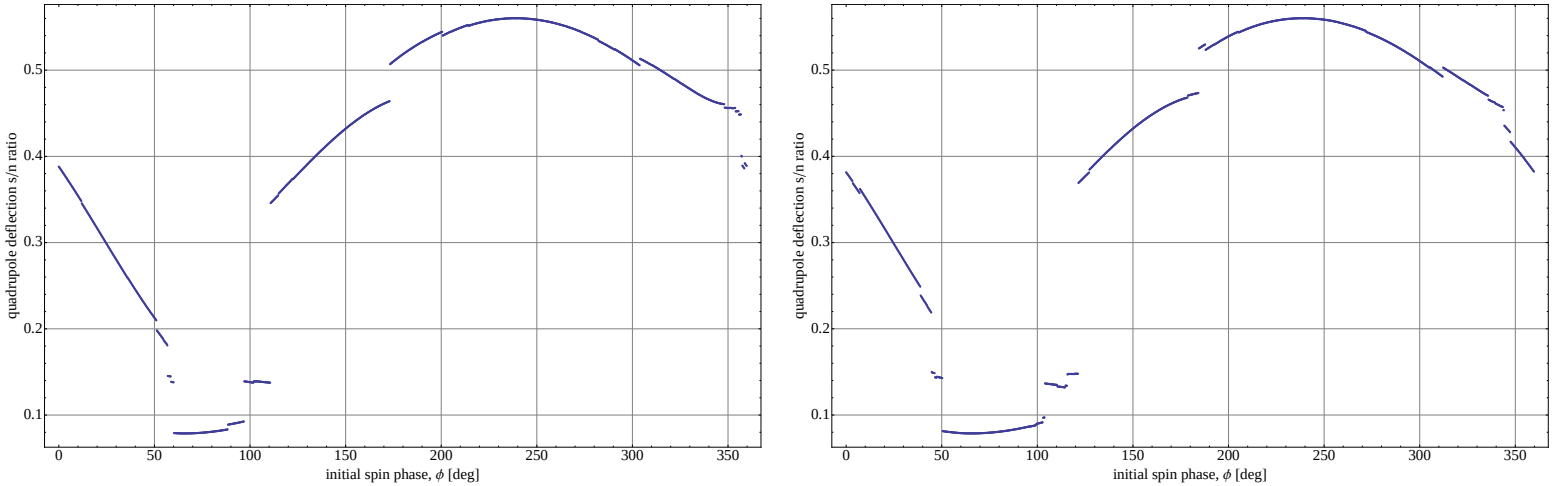


FIGURE 4: Total s/n ratio for the quadrupole deflection for all observations till 31.12.2015 within 10 Jupiter radii. The noise model N_1 was used. The left pane with full FoVs, the right pane with the shrink factor 0.9.

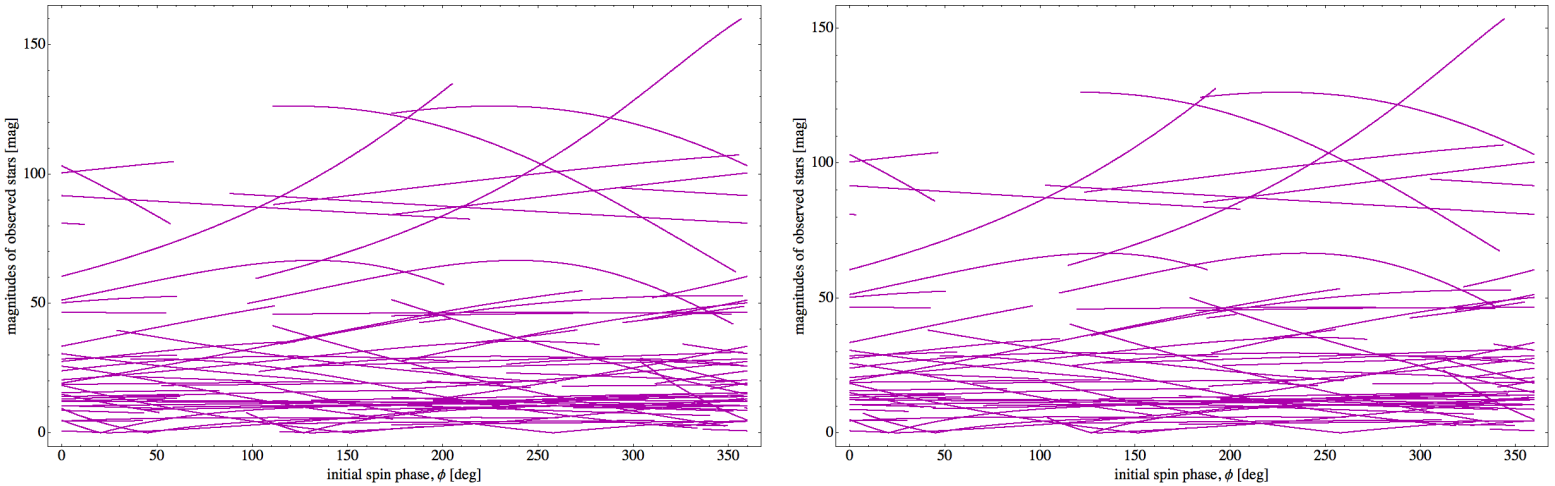


FIGURE 5: S/n ratios for individual observations for the monopole deflection for all observations till 31.12.2015 within 10 Jupiter radii. The noise model N_1 was used. The left pane with full FoVs, the right pane with the shrink factor 0.9.

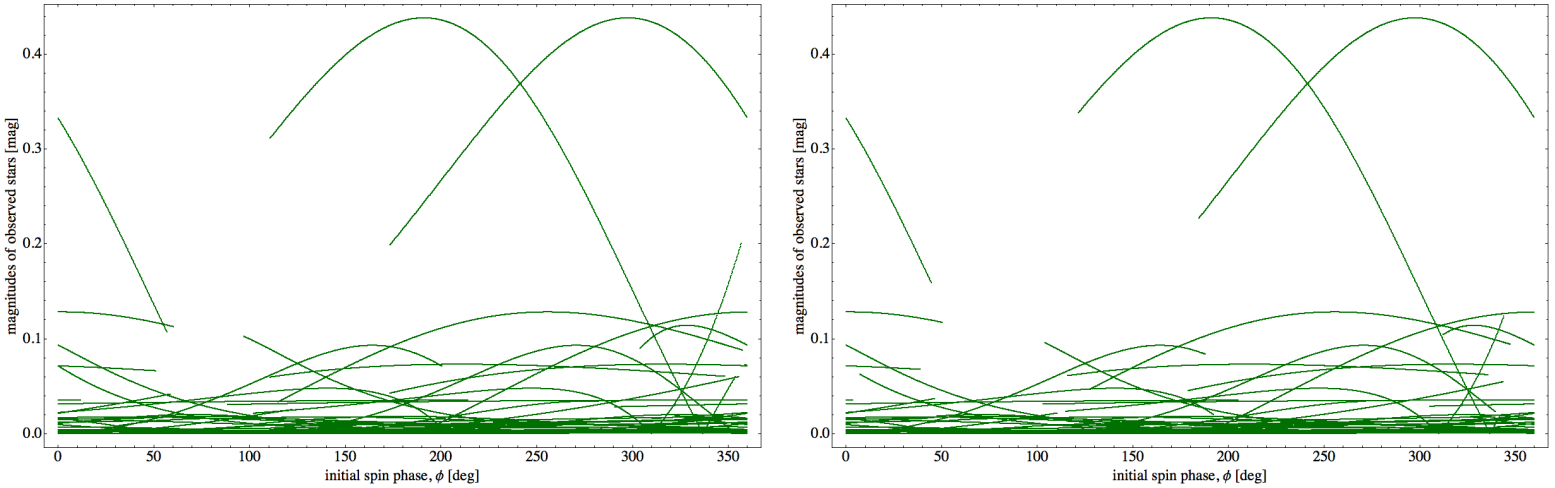


FIGURE 6: S/n ratio for individual observations for the quadrupole deflection for all observations till 31.12.2015 within 10 Jupiter radii. The noise model N_1 was used. The left pane with full FoVs, the right pane with the shrink factor 0.9.

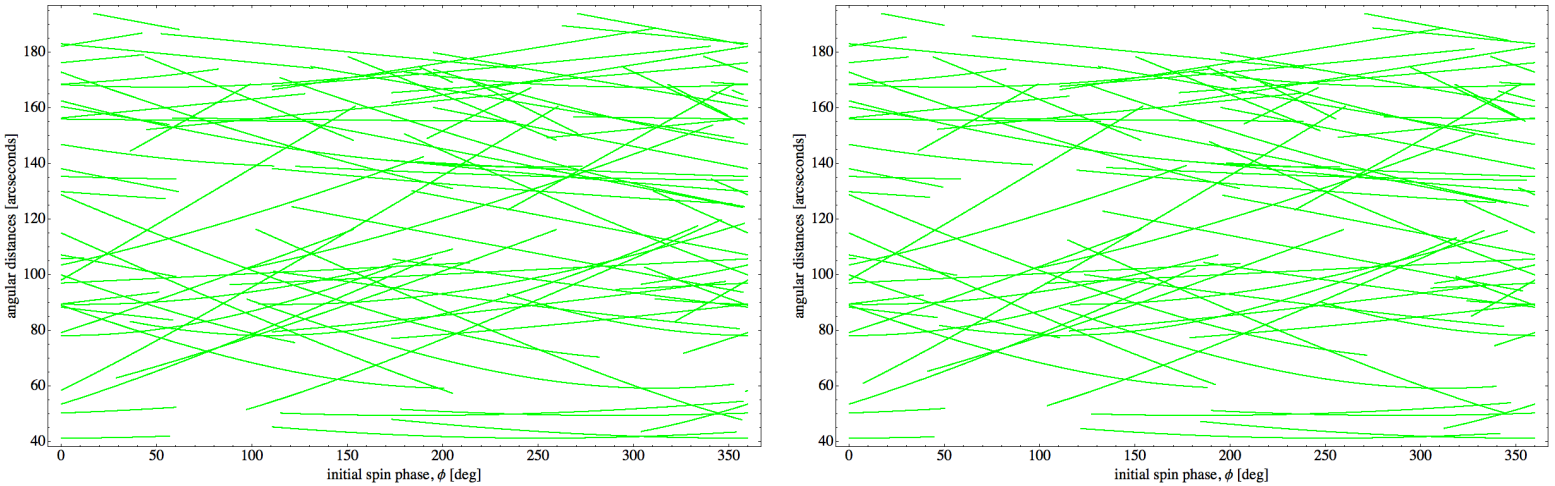


FIGURE 7: The angular distances in arcseconds for all observations till 31.12.2015 within 10 Jupiter radii. The left pane with full FoVs, the right pane with the shrink factor 0.9.

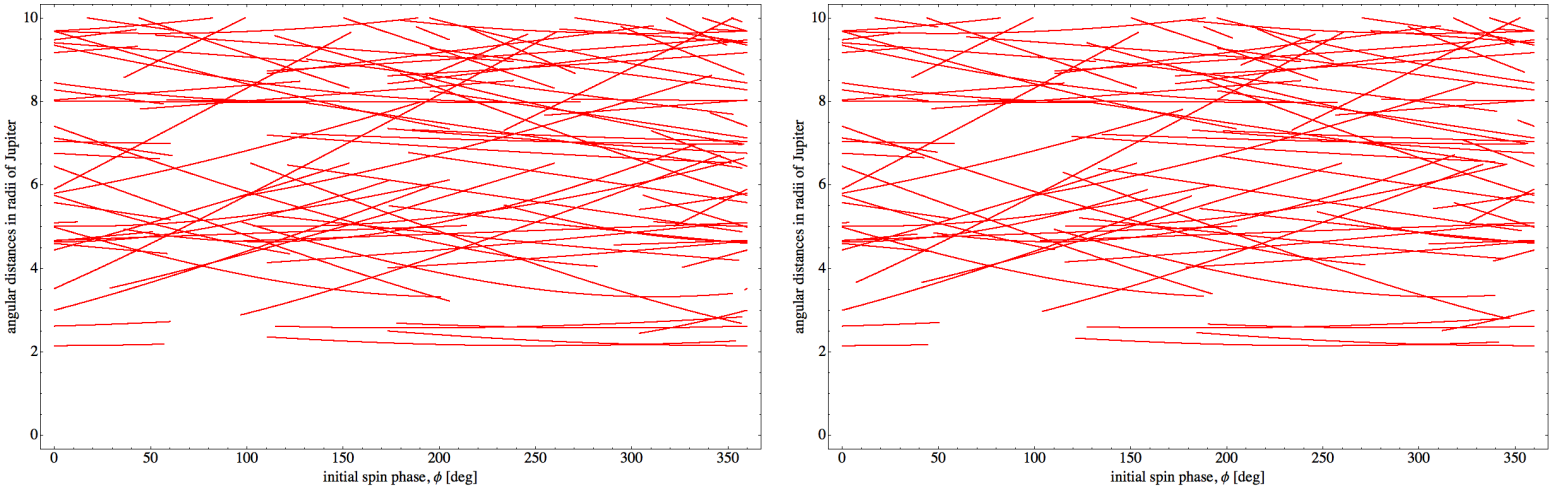


FIGURE 8: The angular distances in Jupiter's radii for all observations till 31.12.2015 within 10 Jupiter radii. The left pane with full FoVs, the right pane with the shrink factor 0.9.

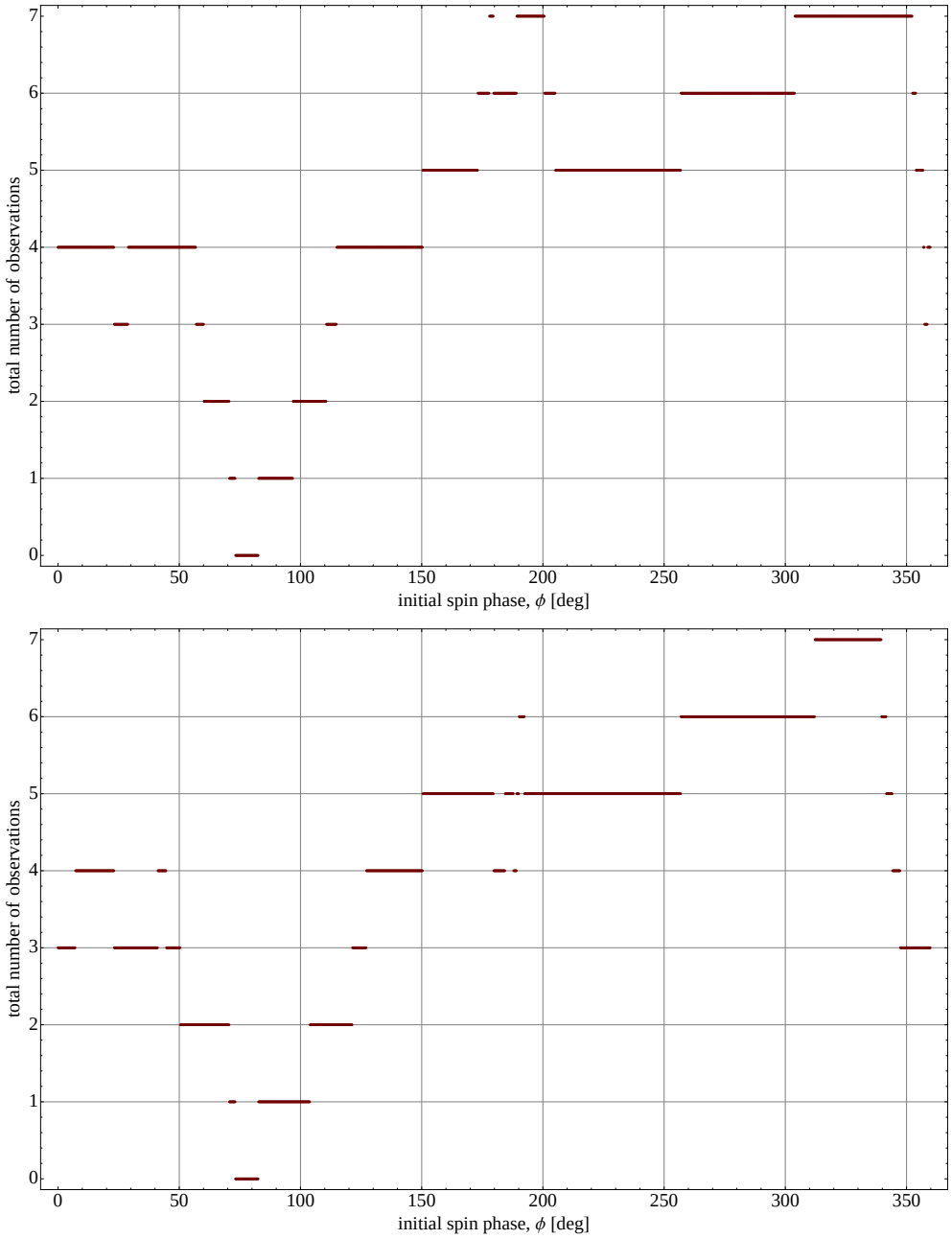


FIGURE 9: Number of observations till 31.12.2015 within 4 Jupiter radii. The upper pane with full FoVs, the lower pane with the shrink factor 0.9.

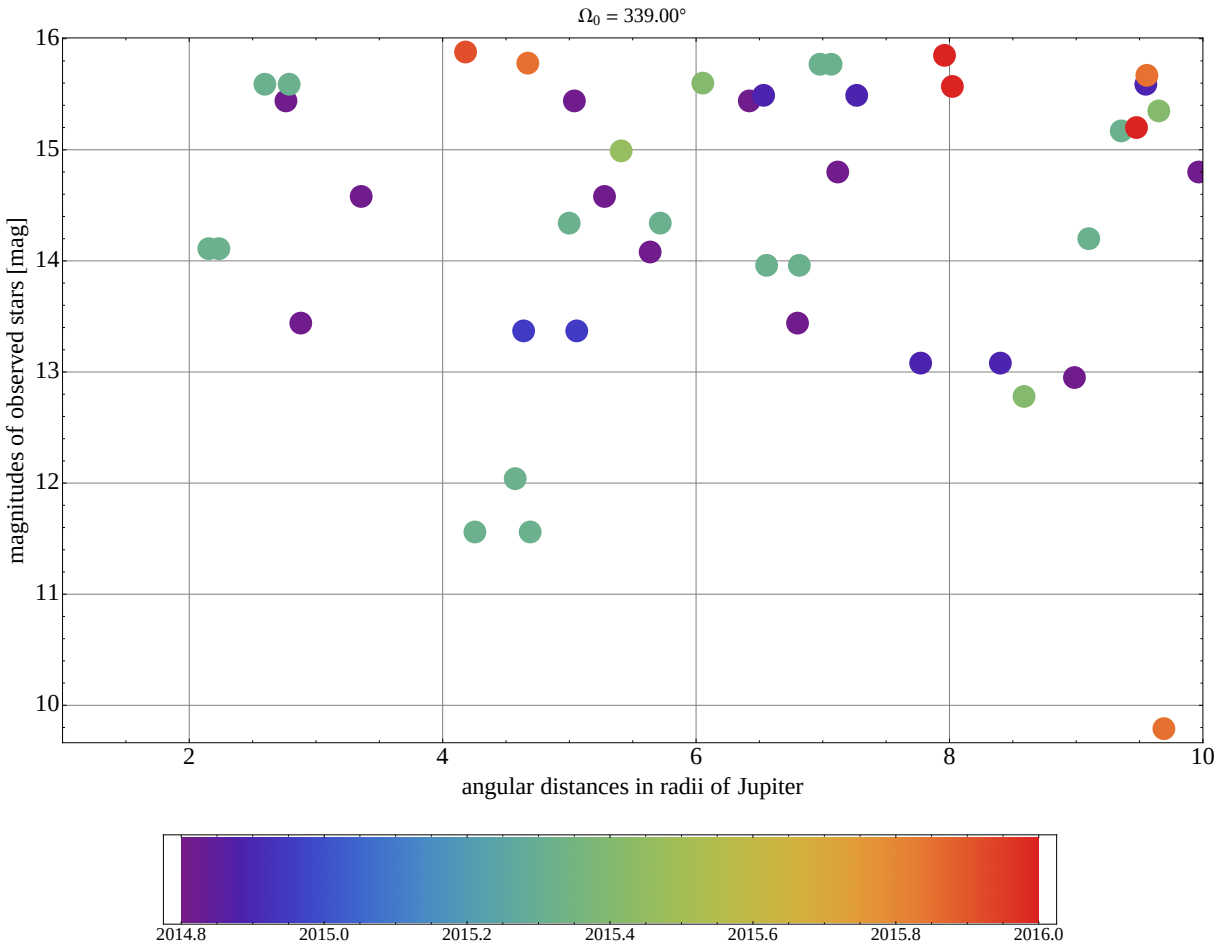


FIGURE 10: Characteristics of individual observations for $\Omega_0 = 339.0°$: each observation corresponds to a circle on the plot. The position of this circle is given by the angular distance in Jupiter's radii at which a star was observed (x-axis) and the magnitude of the observed star (y-axis). The color of the circle corresponds to the time of observation as shown at the bottom of the Figure. The plot for this value of Ω_0 is the same for the shrink factors 1.0 and 0.9.

5 Recommendation of the initial spin phase till the end of 2015

The considerations presented above led us to the following recommendation of the initial spin phase to be used till the end of 2015:

$$\Omega_0 = 339.0^\circ\,. \tag{3}$$

We stress that this choice of the spin phase is optimal for investigating the actual performance of Gaia for observations close to Jupiter and for testing the algorithms and software for the differential GAREQ solution, but it is absolutely not suitable for GAREQ itself starting from January 2016. If no spin phase maneuvers are performed the GAREQ accuracy would be reduced by a significant factor.

Finally, Appendix C gives the time intervals during which GAREQ-relevant observations are performed. These time intervals are valid for any initial spin phase. The time outside of those time intervals can be used for any on-board activities that lead to breaks in scientific operations without disturbing the GAREQ observations.

6 Online repository

The repository with additional data, plots and animations can be found at:

`http://astro.geo.tu-dresden.de/archiveSogarRuns/SpinPhase2015/`

The animation files were tested with the VLC media player (`http://www.videolan.org/vlc/`). The details of the content of the repository can be requested from the authors.

Acknowledgments

This report describes the results of the work which was prepared, discussed, organized and made possible by a large number of people from ESA, MOC, SOC and DPAC. Without contribution of all these people the SL optimization for GAREQ would have been impossible. We would like to explicitly thank Christophe Ordénovic, Guillem Anglada-Escudé, Jos de Bruijne, Lennart Lindegren, Hassan Siddiqui, Ummi Abbas, Mariateresa Crosta and Mario Lattanzi.

SK was partially supported by the BMWi grants 50QG0901 and 50QG1402 awarded by the Deutsche Zentrum für Luft- und Raumfahrt e.V. (DLR).

A Comparison of the latest Gaia orbit with the orbit used to optimize the precession phase

The orbit of Gaia is re-constructed regularly and new versions of the Gaia orbit are delivered by the MOC approximately once per week. The Gaia orbit `ORB1_20131230_000001.txt` used for the optimization of the initial precession phase (Klioner & Mignard, 2014) was delivered on 30 December 2013. The requirement for that orbit was the accuracy of 7000 km in position over the whole mission of 5.5 years. For the SOGAR runs used for the spin phase optimization described in this report, the Gaia orbit `ORB1_20140819_000001.txt` delivered on 19 August 2014 was used. With almost 8 months between the used orbits it is interesting to see the differences in the Gaia position computed with these orbits. Figures 11–12 show the differences in Gaia position between the MOC orbit files delivered on 19 August 2014 and 30 December 2013. We see that the maximal difference does not exceed 7000 km and is so far within the accuracy requirement giving the maximal error of the parallactic effect for Jupiter of about $\sim$10% of the Jupiter radius.

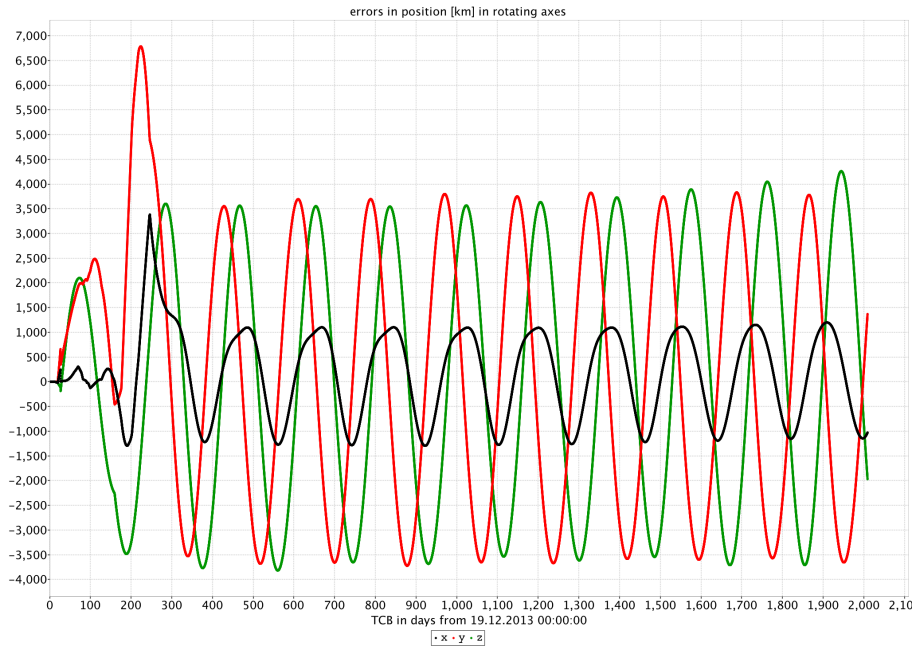


FIGURE 11: Differences (in km) in Gaia position in the X, Y and Z components in the co-rotating coordinates centered at L_2 between the MOC orbit files delivered on 19.08.2014 and 30.12.2013.

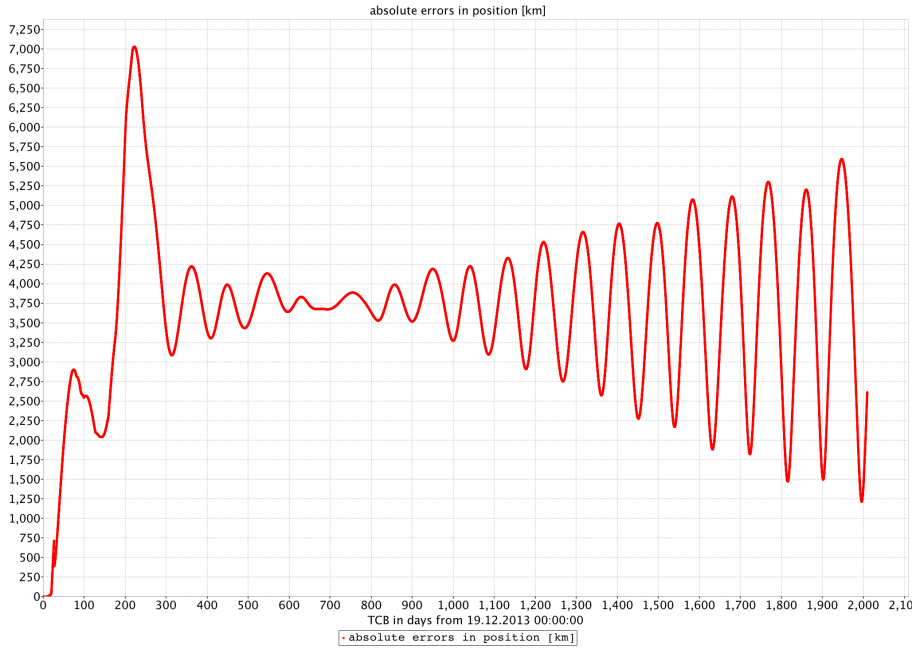


FIGURE 12: Absolute difference in Gaia position (in km) between the MOC orbit files delivered on 19.08.2014 and 30.12.2013.

B Observations for $\nu_0 = 52.66°$ and $\Omega_0 = 339.0°$ till the end of 2015

This Appendix contains the SOGAR output for the observations of stars with magnitudes below 16 within 10 radii of Jupiter and till the end of 2015. Here we show the observations of stars closer than 4 radii of Jupiter.

ra	dec	mag	fov	year	theta/Rp	theta	R_p	ra_p	del_p	eta_p	zeta_p	eta_s	zeta_s	
142.0357	15.5467	13.44	2	2014.812545	2.88019	51.37	17.84	142.04808	15.55459	-0.00121	0.35754	0.01303	0.35852	
142.0456	15.5381	14.58	2	2014.812545	3.35706	59.88	17.84	142.04808	15.55459	-0.00121	0.35754	0.00901	0.37067	
142.0753	15.5351	15.44	1	2014.813027	2.76313	49.31	17.84	142.07068	15.54806	-0.00119	-0.31292	0.00138	-0.29947	
135.4681	17.8629	15.59	1	2015.314122	2.78864	53.59	19.22	135.46670	17.87771	0.00053	-0.35456	-0.01318	-0.34876	*
135.4736	17.8877	14.11	1	2015.314122	2.23397	42.93	19.22	135.46670	17.87771	0.00053	-0.35456	0.00625	-0.36503	**
135.4681	17.8629	15.59	2	2015.314325	2.59662	49.89	19.21	135.47063	17.87653	0.00053	-0.05651	-0.01039	-0.04797	*
135.4736	17.8877	14.11	2	2015.314325	2.15426	41.39	19.21	135.47063	17.87653	0.00053	-0.05651	0.00905	-0.06422	**

Here ra and dec is the right ascension and declination of the star in degrees, mag is its magnitude, year is the observation time in years, fov is the FoV in which the star is observed (1 is the preceding, 2 is the following), theta is the angular distance between the star and the centre of Jupiter in arcseconds, R_p is the angular radius of Jupiter in arcseconds, theta/R_p is the angular distance between the star and Jupiter in Jupiter's radii, ra_p and dec_p is the right ascension and declination of Jupiter in degrees, eta_p and zeta_p are the AL and AC field angles of Jupiter and eta_s and zeta_s are the field angles of the star. The field angles are given in degrees.

We can see that we have 3 observations of three different stars on 23 October 2014 and two compound observations with two observations each on 24 April 2015. Observations that belong to two compound observations are marked with '$\star$' and '$\star\star$', respectively.

Full list of these observations and their details are given on the next page. Additional data fields not explained above are: days is the observation time in days counted from J2010 TCB, eta_ps and zeta_ps are the differences of the AC and AL field angles of the star and Jupiter (in degrees), delf_M and defl_Q is the monopole and quadrupole deflection of light due to Jupiter for the observed star in milliarcseconds, delf_M_al and defl_Q_al is the monopole and quadrupole deflection of light due to Jupiter for the observed star projected on the scan direction (AL direction) in milliarcseconds, fish_M and fish_Q is the Fisher information for the monopole and quadrupole deflections, respectively.

ra	dec	mag	fov	year	days	etat_ps	zeta_ps	theta/Rp	defl_M	defl_M_al	defl_Q	defl_Q_al	fish_M	fish_Q	theta	R_p	ra_p	del_p	eta_p	zeta_p	eta_s	zeta_s
142.0025	15.5620	12.95	2	2014.812545	1757.78199	0.03452	-0.02811	8.98624	1.811e+00	1.404e+00	3.296e-04	3.140e-04	2.190e+03	1.095e-04	160.28	17.84	142.04808	15.55459	-0.00121	0.35754	0.03332	0.32943
142.0357	15.5467	13.44	2	2014.812545	1757.78199	0.01424	0.00098	2.88019	5.649e+00	5.636e+00	1.001e-02	-3.677e-03	2.270e+04	9.663e-03	51.37	17.84	142.04808	15.55459	-0.00121	0.35754	0.01303	0.35852
142.0427	15.5895	14.80	2	2014.812545	1757.78199	-0.01270	-0.03290	7.11820	2.286e+00	-8.230e-01	6.630e-04	-3.942e-04	1.375e+02	3.153e-05	126.96	17.84	142.04808	15.55459	-0.00121	0.35754	-0.01390	0.32464
142.0456	15.5381	14.58	2	2014.812545	1757.78199	0.01022	0.01312	3.35706	4.847e+00	2.977e+00	6.321e-03	-1.520e-03	2.207e+03	5.751e-04	59.88	17.84	142.04808	15.55459	-0.00121	0.35754	0.00901	0.37067
142.0743	15.5203	14.08	2	2014.812545	1757.78199	-0.00509	0.04224	8.58823	1.895e+00	-2.268e-01	3.775e-04	3.255e-04	2.035e+01	4.192e-05	153.18	17.84	142.04808	15.55459	-0.00121	0.35754	-0.00630	0.39979
142.0753	15.5726	15.44	2	2014.812545	1757.78199	-0.03168	-0.00282	6.42002	2.534e+00	-2.524e+00	9.038e-04	3.828e-04	7.122e+02	1.638e-05	114.51	17.84	142.04808	15.55459	-0.00121	0.35754	-0.03289	0.35472
142.0753	15.5351	15.44	2	2014.812545	1757.78199	-0.01323	0.02987	6.59405	2.467e+00	-9.993e-01	8.340e-04	1.239e-04	1.116e+02	1.715e-06	117.61	17.84	142.04808	15.55459	-0.00121	0.35754	-0.01444	0.38742
142.0357	15.5467	13.44	1	2014.813027	1757.95814	0.02990	-0.01557	6.80092	2.392e+00	2.122e+00	7.602e-04	7.238e-04	3.218e+03	3.744e-04	121.36	17.84	142.07068	15.54806	-0.00119	-0.31292	0.02871	-0.32850
142.0427	15.5895	14.80	1	2014.813027	1757.95814	0.00280	-0.04932	9.96670	1.633e+00	9.253e-02	2.416e-04	-2.269e-04	1.737e+00	1.044e-05	177.85	17.84	142.07068	15.54806	-0.00119	-0.31292	0.00161	-0.36225
142.0456	15.5381	14.58	1	2014.813027	1757.95814	0.02594	-0.00341	5.27739	3.083e+00	3.057e+00	1.627e-03	3.413e-04	2.326e+03	2.900e-05	94.17	17.84	142.07068	15.54806	-0.00119	-0.31292	0.02475	-0.31633
142.0743	15.5203	14.08	1	2014.813027	1757.95814	0.01077	0.02579	5.63755	2.886e+00	1.112e+00	1.335e-03	7.143e-04	4.892e+02	2.018e-04	100.60	17.84	142.07068	15.54806	-0.00119	-0.31292	0.00958	-0.28714
142.0753	15.5726	15.44	1	2014.813027	1757.95814	-0.01604	-0.01915	5.03953	3.229e+00	-2.073e+00	1.868e-03	6.234e-04	4.802e+02	4.343e-05	89.93	17.84	142.07068	15.54806	-0.00119	-0.31292	-0.01723	-0.33208
142.0753	15.5351	15.44	1	2014.813027	1757.95814	0.00257	0.01345	2.76313	5.889e+00	1.105e+00	1.134e-02	1.050e-02	1.365e+02	1.233e-02	49.31	17.84	142.07068	15.54806	-0.00119	-0.31292	0.00138	-0.29947
144.6204	14.8496	15.59	1	2014.889654	1785.94613	-0.04385	-0.02683	9.54959	1.704e+00	-1.453e+00	2.746e-04	-2.719e-04	2.051e+02	7.181e-06	185.08	19.38	144.66509	14.82175	-0.00063	-0.32600	-0.04448	-0.35283
144.6240	14.8087	13.08	1	2014.889654	1785.94613	-0.00550	-0.04148	7.77239	2.093e+00	-2.753e-01	5.093e-04	4.814e-04	7.553e+01	2.309e-04	150.63	19.38	144.66509	14.82175	-0.00063	-0.32600	-0.00613	-0.36748
144.6293	14.8282	15.49	1	2014.889654	1785.94613	-0.02079	-0.02837	6.53324	2.491e+00	-1.472e+00	8.576e-04	-2.230e-04	2.311e+02	5.304e-06	126.62	19.38	144.66509	14.82175	-0.00063	-0.32600	-0.02142	-0.35437
144.6240	14.8087	13.08	2	2014.889857	1786.02014	-0.00802	-0.04452	8.40143	1.937e+00	-3.431e-01	4.032e-04	3.589e-04	1.173e+02	1.284e-04	162.86	19.39	144.66907	14.82076	-0.00063	-0.01401	-0.00865	-0.05853
144.6293	14.8282	15.49	2	2014.889857	1786.02014	-0.02332	-0.03143	7.26786	2.239e+00	-1.334e+00	6.229e-04	-1.738e-04	1.897e+02	3.221e-06	140.89	19.39	144.66907	14.82076	-0.00063	-0.01401	-0.02395	-0.04544
145.0572	14.7764	13.37	2	2014.951450	1808.51724	0.02686	-0.01135	5.05841	3.217e+00	2.963e+00	1.847e-03	1.279e-03	6.692e+03	1.248e-03	104.98	20.75	145.08654	14.78317	0.00161	0.32588	0.02847	0.31452
145.0572	14.7764	13.37	1	2014.951933	1808.69340	0.02557	-0.00790	4.63901	3.507e+00	3.351e+00	2.395e-03	1.106e-03	8.562e+03	9.321e-04	96.32	20.76	145.08342	14.78499	0.00164	-0.28322	0.02721	-0.29112
135.4387	17.8798	14.34	1	2015.314122	1940.98319	0.01428	0.02254	4.99863	3.255e+00	1.743e+00	1.915e-03	1.400e-04	9.442e+02	6.094e-06	96.06	19.22	135.46670	17.87771	0.00053	-0.35456	0.01482	-0.33202
135.4525	17.8430	15.77	1	2015.314122	1940.98319	-0.02428	0.02825	6.97800	2.332e+00	-1.520e+00	7.038e-04	4.032e-04	1.894e+02	1.333e-05	134.10	19.22	135.46670	17.87771	0.00053	-0.35456	-0.02375	-0.32631
135.4606	17.8997	11.56	1	2015.314122	1940.98319	0.02212	-0.00516	4.25444	3.824e+00	3.724e+00	3.105e-03	-1.847e-03	1.132e+04	2.784e-03	81.76	19.22	135.46670	17.87771	0.00053	-0.35456	0.02265	-0.35972
135.4668	17.9127	13.96	1	2015.314122	1940.98319	0.03087	-0.01649	6.55685	2.481e+00	2.189e+00	8.483e-04	-8.388e-04	2.118e+03	3.110e-04	126.00	19.22	135.46670	17.87771	0.00053	-0.35456	0.03141	-0.37105
135.4681	17.8629	15.59	1	2015.314122	1940.98319	-0.01371	0.00580	2.78864	5.835e+00	-5.373e+00	1.103e-02	1.007e-02	2.803e+03	9.842e-03	53.59	19.22	135.46670	17.87771	0.00053	-0.35456	-0.01318	-0.34876
135.4736	17.8877	14.11	1	2015.314122	1940.98319	0.00572	-0.01046	2.23397	7.283e+00	3.493e+00	2.145e-02	4.166e-04	4.695e+03	6.678e-05	42.93	19.22	135.46670	17.87771	0.00053	-0.35456	0.00625	-0.36503
135.4912	17.8911	12.04	1	2015.314122	1940.98319	0.00092	-0.02686	5.03518	3.232e+00	1.110e-01	1.873e-03	1.851e-03	1.368e+01	3.808e-03	96.76	19.22	135.46670	17.87771	0.00053	-0.35456	0.00145	-0.38142
135.5074	17.9102	14.20	1	2015.314122	1940.98319	0.01048	-0.04945	9.47043	1.718e+00	3.561e-01	2.816e-04	2.195e-04	4.489e+01	1.705e-05	182.00	19.22	135.46670	17.87771	0.00053	-0.35456	0.01101	-0.40402
135.4387	17.8798	14.34	2	2015.314325	1941.05719	0.01706	0.02530	5.71747	2.846e+00	1.592e+00	1.279e-03	2.045e-04	7.877e+02	1.300e-05	109.85	19.21	135.47063	17.87653	0.00053	-0.05651	0.01759	-0.03122
135.4525	17.8430	15.77	2	2015.314325	1941.05719	-0.02150	0.03098	7.06562	2.303e+00	-1.313e+00	6.779e-04	1.996e-04	1.414e+02	3.268e-06	135.75	19.21	135.47063	17.87653	0.00053	-0.05651	-0.02098	-0.02553
135.4606	17.8997	11.56	2	2015.314325	1941.05719	0.02492	-0.00240	4.69074	3.469e+00	3.453e+00	2.317e-03	-5.474e-04	9.732e+03	2.446e-04	90.12	19.21	135.47063	17.87653	0.00053	-0.05651	0.02544	-0.05891
135.4668	17.9127	13.96	2	2015.314325	1941.05719	0.03369	-0.01372	6.81510	2.387e+00	2.211e+00	7.555e-04	-6.770e-04	2.161e+03	2.026e-04	130.94	19.21	135.47063	17.87653	0.00053	-0.05651	0.03421	-0.07023
135.4681	17.8629	15.59	2	2015.314325	1941.05719	-0.01091	0.00854	2.59662	6.266e+00	-4.935e+00	1.366e-02	1.273e-02	2.365e+03	1.573e-02	49.89	19.21	135.47063	17.87653	0.00053	-0.05651	-0.01039	-0.04797
135.4736	17.8877	14.11	2	2015.314325	1941.05719	0.00853	-0.00771	2.15426	7.553e+00	5.601e+00	2.392e-02	-1.993e-02	1.207e+04	1.527e-01	41.39	19.21	135.47063	17.87653	0.00053	-0.05651	0.00905	-0.06422
135.4912	17.8911	12.04	2	2015.314325	1941.05719	0.00374	-0.02411	4.57270	3.558e+00	5.456e-01	2.501e-03	2.182e-03	3.308e+02	5.288e-03	87.85	19.21	135.47063	17.87653	0.00053	-0.05651	0.00427	-0.08063
135.5074	17.9102	14.20	2	2015.314325	1941.05719	0.01331	-0.04670	9.09942	1.788e+00	4.903e-01	3.174e-04	2.017e-04	8.509e+01	1.440e-05	174.83	19.21	135.47063	17.87653	0.00053	-0.05651	0.01384	-0.10321
135.5211	17.8901	15.17	2	2015.314325	1941.05719	-0.01048	-0.04882	9.35547	1.739e+00	-3.650e-01	2.921e-04	2.435e-04	1.916e+01	8.527e-06	179.74	19.21	135.47063	17.87653	0.00053	-0.05651	-0.00995	-0.10533
138.7815	16.8592	15.60	1	2015.407840	1975.21342	-0.02885	0.00470	6.05287	2.688e+00	-2.653e+00	1.078e-03	-2.474e-04	6.771e+02	5.888e-06	105.23	17.39	138.80950	16.87091	0.00127	-0.04684	-0.02758	-0.04214
138.8065	16.9123	12.78	1	2015.407840	1975.21342	0.02001	0.03633	8.58834	1.895e+00	9.138e-01	3.775e-04	1.166e-04	9.278e+02	1.510e-05	149.32	17.39	138.80950	16.87091	0.00127	-0.04684	0.02128	-0.01051
138.8276	16.9142	15.35	1	2015.407840	1975.21342	0.03796	0.02705	9.65190	1.686e+00	1.373e+00	2.660e-04	-2.281e-04	2.291e+02	6.326e-06	167.81	17.39	138.80950	16.87091	0.00127	-0.04684	0.03923	-0.01979
141.6950	15.9767	14.99	1	2015.459186	1993.96753	-0.00225	-0.02487	5.40862	3.008e+00	-2.707e-01	1.511e-03	1.078e-03	1.246e+01	1.976e-04	89.91	16.62	141.66916	15.97454	-0.00167	0.25102	-0.00392	0.22615
169.3749	5.7074	15.67	2	2015.855772	2138.82078	0.00808	-0.04398	9.55777	1.702e+00	3.077e-01	2.737e-04	-1.569e-04	8.530e+00	2.217e-06	160.98	16.84	169.40500	5.67424	-0.00177	0.38654	0.00632	0.34256
169.4203	5.6448	15.78	1	2015.856254	2138.99693	0.01904	0.01075	4.67206	3.483e+00	3.033e+00	2.344e-03	-2.157e-03	7.472e+02	3.779e-04	78.72	16.85	169.43073	5.66407	-0.00174	-0.17310	0.01730	-0.16235
169.4691	5.6396	9.79	1	2015.856254	2138.99693	-0.01931	0.04105	9.69211	1.679e+00	-7.148e-01	2.625e-04	-4.692e-05	4.171e+02	1.797e-06	163.31	16.85	169.43073	5.66407	-0.00174	-0.17310	-0.02105	-0.13206
172.1692	4.5823	15.88	1	2015.915800	2160.74596	0.02032	0.00404	4.18082	3.892e+00	3.817e+00	3.270e-03	1.883e-03	1.077e+03	2.622e-04	74.57	17.84	172.15836	4.59991	0.00070	0.24424	0.02102	0.24828
174.0289	3.9193	15.20	1	2015.995158	2189.73129	0.04679	-0.02082	9.47590	1.717e+00	1.569e+00	2.808e-04	2.496e-04	3.442e+02	8.714e-06	184.38	19.46	174.08021	3.91946	0.00098	-0.16936	0.04777	-0.19018
174.0850	3.9626	15.57	1	2015.995158	2189.73129	-0.02200	-0.03737	8.02269	2.028e+00	-1.029e+00	4.627e-04	-6.233e-05	1.048e+02	3.844e-07	156.10	19.46	174.08021	3.91946	0.00098	-0.16936	-0.02102	-0.20672
174.1202	3.9033	15.85	1	2015.995158	2189.73129	-0.02979	0.03104	7.96076	2.044e+00	-1.415e+00	4.736e-04	-3.664e-04	1.523e+02	1.021e-05	154.90	19.46	174.08021	3.91946	0.00098	-0.16936	-0.02882	-0.13831

C Time periods of GAREQ-relevant observations for $\nu_0 = 52.66°$

Using the currently available orbital data we computed the time intervals during which all GAREQ-relevant observations of stars with magnitudes up to 16 within 10 radii of Jupiter and for the initial precession phase $\nu_0 = 52.66°$ take place. The time intervals are computed to cover observations for any initial spin phases. These time intervals depend on the updates of the Gaia orbit only weakly. The following list can therefore be used consulted to check which time intervals are important for GAREQ-relevant observations. Obviously, before making important decisions on scheduling of on-board activities leading to breaks in scientific observation this list should be updated.

24.10.2014 - 25.10.2014
21.11.2014 - 23.11.2014
14.12.2014 - 15.12.2014
25.04.2015 - 27.04.2015
30.05.2015 - 31.05.2015
17.06.2015 - 19.06.2015
09.11.2015 - 11.11.2015
01.12.2015 - 02.12.2015
30.12.2015 - 31.12.2015
11.05.2016 - 12.05.2016
08.06.2016 - 09.06.2016
04.07.2016 - 05.07.2016
26.11.2016 - 27.11.2016
09.12.2016 - 10.12.2016
13.01.2017 - 15.01.2017
22.02.2017 - 27.02.2017
29.05.2017 - 30.05.2017
18.06.2017 - 19.06.2017
20.07.2017 - 22.07.2017
29.01.2018 - 30.01.2018
28.02.2018 - 02.03.2018
19.03.2018 - 21.03.2018
19.06.2018 - 21.06.2018
25.06.2018 - 27.06.2018
05.08.2018 - 07.08.2018
12.09.2018 - 13.09.2018
25.09.2018 - 27.09.2018
13.02.2019 - 14.02.2019
10.03.2019 - 11.03.2019
06.04.2019 - 07.04.2019